Thin Solid Films 520 (2012) 4580–4585

Contents lists available at SciVerse ScienceDirect

Thin Solid Films

journal homepage: www.elsevier.com/locate/tsf

Effect of the nanostructure on room temperature ferromagnetism and resistivity of undoped ZnO thin films grown by chemical vapor deposition

Lidia I. Burova [a,*], Nikolai S. Perov [b], Anna S. Semisalova [b], Vladimir A. Kulbachinskii [b], Vladimir G. Kytin [b], Vladimir V. Roddatis [c], Alexander L. Vasiliev [c,d], Andrey R. Kaul [a]

[a] Laboratory of Coordination Chemistry, Division of Inorganic Chemistry, Department of Chemistry, Lomonosov Moscow State University, Leninskie Gory, Moscow 119991, Russia
[b] Faculty of Physics, Lomonosov Moscow State University, Leninskie Gory, Moscow 119991, Russia
[c] National Research Center "Kurchatov Institute", Akademika Kurchatova sq. 1, Moscow, 123182, Russia
[d] Institute of Crystallography RAS, Leninskii pr., 59, Moscow 119333, Russia

ARTICLE INFO

Available online 10 November 2011

Keywords:
Undoped ZnO
Nanostructure
Thin films
Room-temperature ferromagnetism
Water-assisted MOCVD
Epitaxial variant structure

ABSTRACT

Undoped zinc oxide thin films having various types of morphology and nanostructure were deposited by metal organic chemical vapor deposition (MOCVD) on single-crystalline substrates. Water-assisted MOCVD process at low temperatures (300–500 °C) was applied along with conventional MOCVD in oxygen-containing atmosphere at 500 and 600 °C. The strong correlation between room-temperature ferromagnetism of the films, their electrical properties and morphology at nano-scale was demonstrated.

1. Introduction

Ferromagnetism of zinc oxide, both undoped and doped with transition metals, is an astonishing phenomenon and subject of much controversy. Since Dietl at al. [1] theoretically predicted in 2000 weak room-temperature ferromagnetism (RTFM) of ZnO doped with transition metals (TM), many researchers have obtained ferromagnetic ZnO films doped with Co, Mn and other TM with T_c close to room temperature [2–6]. However, there are several reports that deny even the possibility of intrinsic RTFM in zinc oxide [7–9]. Despite the large number of publications on this subject, the nature of magnetism in ZnO films is still not clear. One of the main open questions today is the role of TM-doping in the origin of ZnO ferromagnetism [10]. Our Co-doped ZnO films obtained by water-assisted metal organic chemical vapor deposition (MOCVD) [11] showed ferromagnetic behavior at room temperature. However, no logical correlation between the dopant concentration and saturation magnetization of the films was found. Some researchers have reported ferromagnetism in Mn-doped ZnO [12,13], while others reported antiferromagnetism or paramagnetism [14,15]. Even in the films exhibiting RTFM, their saturation magnetization depends very non-monotonically on Mn concentration [16]. To date, many scientists have suggested that TM-doping does not play the key role in ferromagnetism of zinc oxide, and that ZnO can be ferromagnetic without any doping [17–21]. In this case, however, the origin of RTFM becomes even less explicable. In different papers defects in ZnO, such as oxygen vacancies, zinc vacancies or interstitials, are suggested to be responsible for FM. Unfortunately, the conclusive evidence of this fact does not exist yet. Recently, Prof. Rao's group reported robust RTFM in nanoparticles of several oxides, such as CeO_2, Al_2O_3, In_2O_3, SnO_2, and ZnO [22], which do not possess RTFM in bulk. It was suggested that the exchange interaction between unpaired electron spins arising from oxygen vacancies at the surface of the nanoparticles might be the origin of their ferromagnetism. Furthermore, the authors [23] proposed this type of ferromagnetism arising from surface defects as a universal feature of inorganic nanoparticles. For ZnO in particular, Straumal and coworkers [24] suggest that FM originates through crystallographic imperfections such as grain boundaries in nanogranular ZnO samples and that the magnetic moments are located at the vacancies present at the grain boundaries. In general, it seems that the nanosized state – whether in form of nanoparticles or nanograins – is necessary for zinc oxide to be ferromagnetic. The aim of this study was to reveal the dependence of the magnetic properties of undoped ZnO thin films deposited by CVD on their nanostructure, morphology and defect structure.

2. Experimental section

The films were deposited in a laboratory scale hot-wall MOCVD apparatus. Single-crystalline hexagonal (1–102) Al_2O_3 (r-sapphire), (0001) Al_2O_3 (c-sapphire), cubic (111) $ZrO_2(Y_2O_3)$ (yttrium stabilized zirconia, YSZ) and (111) $MgAl_2O_4$ substrates were used. All substrates were subjected to ultrasound-assisted acetone washing for 10 min before deposition. Volatile MOCVD precursor – Zn acetylacetonate

* Corresponding author. Tel./fax: +7 495 939 1492.
E-mail address: burova@inorg.chem.msu.ru (L.I. Burova).

0040-6090/$ – see front matter
doi:10.1016/j.tsf.2011.10.198

Table 1
Deposition parameters and the main results on magnetic properties and structure of the deposited ZnO films.

Sample	Substrate	Deposition temperature and reacting gas	Film thickness (nm)	XRD data and film morphology	Magnetic properties at RT
R_Ox	(1–102) Al_2O_3	600 °C, oxygen	140	Dense, flat epitaxial film with micro-sized whiskers on the top	Non-magnetic
C_Ox	(0001) Al_2O_3	600 °C, oxygen	280	The same as R_Ox	Non-magnetic
Y_Ox	(111) $ZrO_2(Y_2O_3)$	600 °C, oxygen	100	The same as R_Ox	Not measured
MAO_Ox_600	(111) $MgAl_2O_4$	600 °C, oxygen	230	Epitaxial film with in-plane variant structure	Ferromagnetic
MAO_Ox_500	(111) $MgAl_2O_4$	500 °C, oxygen	50	Epitaxial film with in-plane variant structure	Ferromagnetic
R_W_300	(1–102) Al_2O_3	300 °C, water vapor	110	Polycrystalline film	Ferromagnetic
R_W_500	(1–102) Al_2O_3	500 °C, water vapor	150	Polycrystalline film	Ferromagnetic

$(Zn(acac)_2)$ – was synthesized in our laboratory using conventional methodic from Zn nitrate tetrahydrate ("Reachim"; Fe, Mn, Cu≤ 10 ppm), dehydrated acetylacetone and KOH (pro analyse). As-synthesized $Zn(acac)_2 * xH_2O$ $(x = 1 \div 2)$ was than dehydrated and additional purified by vacuum sublimation. The substrates were attached to the holder with Ta wire; Ta foil was used as an extra nonmagnetic protecting layer between the nonmagnetic stainless steel holder and the substrates. The deposition temperature was controlled by a thermocouple placed near the substrate. $Zn(acac)_2$ was evaporated in the powder flash evaporation system described elsewhere [25] at 220 °C. Argon was used as a carrier gas (10 l/h). When oxygen was used as an oxidizing agent (5 l/h), the deposition temperature was fixed at 500–600 °C.

Water-assisted MOCVD with water vapor as a hydrolyzing agent was used as an alternative technique [11]. In this case heated water vapor was added to the precursor gas directly above the substrate surface, no oxygen was added to the gas mixture. The deposition temperature was in the range 300–500 °C. The water vapor flow rate was controlled by injecting liquid ionized water into the vacuum evaporator using an injection valve with subsequent immediate evaporation of the water. The total pressure in both oxygen-assisted and water-assisted versions of the process was 0.5 kPa. The deposition time was 30–40 min; the deposition rates amounted to 3–7 nm/min. The films prepared were characterized by X-ray diffraction (XRD) using Rigaku Smartlab four-circle diffractometer. θ–2θ scans and φ-scans were measured. Reflections of the substrate were used as internal standard. The morphology of the films was studied by scanning electron microscopy (SEM) with LEO SUPRA 50VP (Carl Zeiss) microscope, operating voltage 15 kV. For the investigation of the nanostructure of ZnO film deposited on the (111) $MgAl_2O_4$ spinel substrate, high-resolution transmission electron microscopy (HRTEM) was employed. The sample was studied using Titan 80-300 TEM/STEM (FEI, Oregon, US) equipped with a spherical aberration (C_s) corrector (electron probe corrector), a high angle annular dark field detector, an atmospheric thin-window energy dispersive spectrometer (Phoenix System, EDAX, Mahwah, NJ, USA), and a post-column energy filter (Gatan,

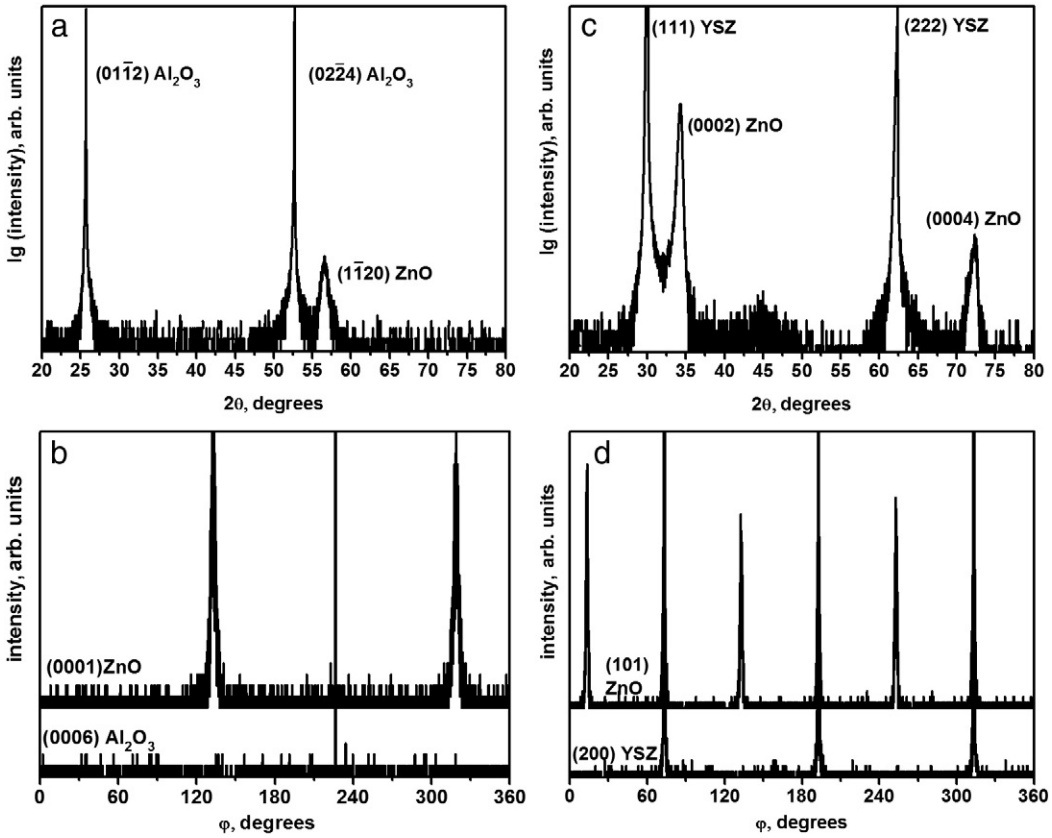

Fig. 1. XRD patterns of **R_Ox** and **Y_Ox** samples: θ–2θ scans of ZnO, (a) and (c) and φ-scans for ZnO and a substrate, (b) and (d), respectively.

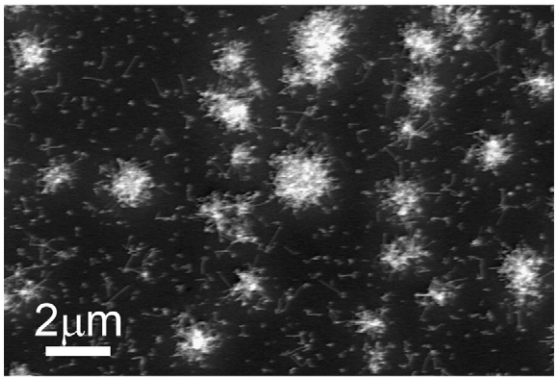

Fig. 2. SEM image of the film deposited at 600 °C by oxygen-assisted CVD on r-sapphire substrate (**R_Ox**).

Pleasanton, CA, US). The TEM was operated at 300 kV. Focused ion beam (FIB)/scanning electron microscope HELIOS (FEI, USA) was used for the cross-sections preparation. The energy of $Ga^{\pm}$ ions was 30 kV in the beginning steps and 2 kV and low ion current in the final (polishing) steps. The cross-sections were handled with micromanipulator (Omniprobe, USA) in-situ in the FIB/SEM. The film magnetization (M) was investigated using vibrating sample magnetometer Lake Shore 7400 with sensitivity up to 1×10^{-9} A∗m^2 in magnetic field (H) up to 1.6 T. A liquid nitrogen flow cryostat was used to carry out the measurements in the temperature range 80–300 K. The signals of diamagnetic sample holders and the substrates were subtracted from the measured signals; the resulting M vs. H curves were fitted with the least-squares method. The temperature dependences of resistivity in the 4.2–295 K temperature range were measured in a home-made automated experimental setup containing a cryostat. Conventional four-probe method in the constant current mode was used. Pb–Sn alloy contacts with typical diameter less than 0.3 mm were soldered to the films. The sample current was held constant with the accuracy 0.05%. The typical dimensions of the samples in these experiments were 4–6 mm length and 1–2 mm width.

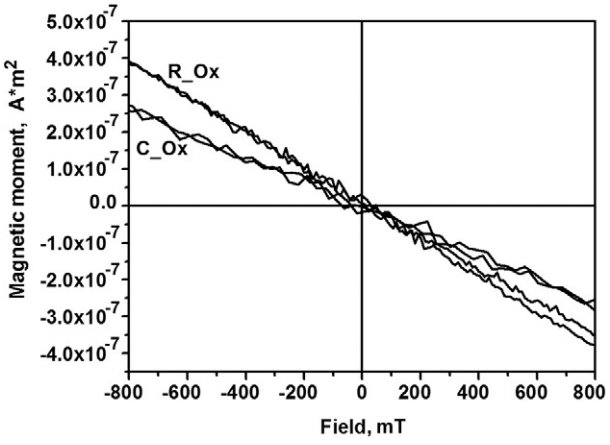

Fig. 3. M(H) at room temperature for the films deposited at 600 °C by oxygen-assisted CVD on r-sapphire (**R_Ox**) and c-sapphire (**C_Ox**) substrates.

3. Results and discussion

The main results on magnetic properties and structure characterization are briefly summarized in Table 1 together with important deposition parameters; below the results are discussed in details.

Undoped ZnO films were deposited on r- and c-sapphire substrates, which are usually used for ZnO deposition, as well as on (111) YSZ substrate using the conventional oxygen-assisted CVD process at 600 °C. We have shown earlier [26] that such conditions result in the deposition of dense, well-crystallized epitaxial films. XRD θ–2θ and φ-scans (Fig. 1) confirmed the epitaxial growth of ZnO with only one in-plane orientation. A representative SEM image of a film obtained under these conditions (**R_Ox** sample) is shown in Fig. 2. The films possessed dense and rather flat surface with micro-sized whiskers, which tend to grow on top of ZnO films due to the high growth anisotropy of zinc oxide.

Magnetization versus magnetic field (M(H)) curves of ZnO films on r- and c-sapphire substrates (**R_Ox** and **C_Ox** samples listed in Table 1) are shown in Fig. 3. The films did not show any ferromagnetism. Only diamagnetic signal from the substrate is present (due to the strong paramagnetism of YSZ, no magnetic measurements could be performed for the films on these substrates).

The morphology of ZnO films deposited in the presence of water vapor was quite different from that of ZnO films deposited in the presence of oxygen. SEM images of the films obtained by water-assisted CVD at 300 and 500 °C are shown in Fig. 4 a) and b), respectively. The films deposited at 300 °C had nano-sized, "crossed plates"-like structure. They consisted of uniform plates, with the plate surface perpendicular to the substrate surface; the characteristic dimensions of the plate edges parallel to the substrate surface being 10×100 nm. The films deposited at 500 °C possessed nano-sized whisker structure. Each whisker itself consisted of planes connected in series. The planes were 200–300 nm wide having hexagonal shape. Under the "whisker layer" we observed a bottom layer of film with granular structure consisting of grains about 20 nm.

Representative room temperature M(H) curves of the ZnO films deposited in the presence of water vapor at 300 and 500 °C on r-sapphire substrates are shown in Fig. 5. The diamagnetic contribution from the substrate and the signal from the sample holder are subtracted. A ferromagnetic behavior with a weak but distinguishable magnetic moment and saturation magnetization of about $2*10^{-8}$ A∗m^2 was observed in the films obtained at 300 °C (**R_W_300**). This value corresponds to 0.65 A∗m^2/kg (0.65 emu/g) and is comparable with values mentioned

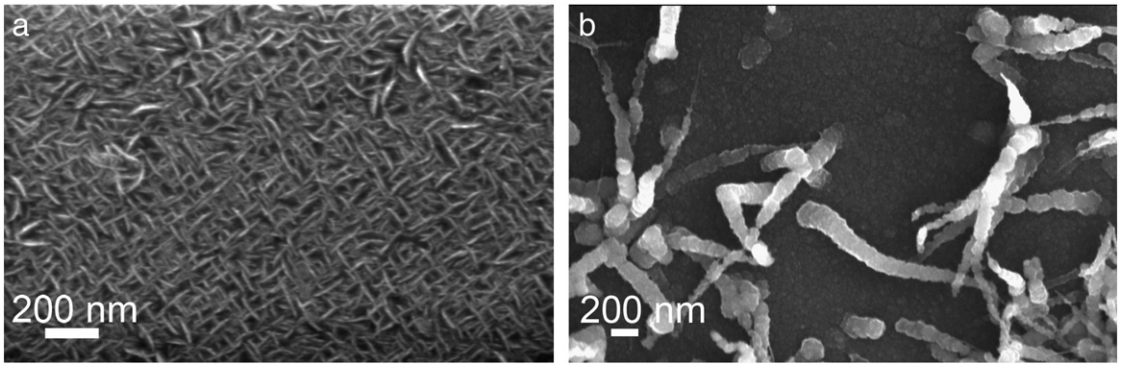

Fig. 4. SEM images of the films deposited by water-assisted CVD on r-sapphire: a) at 300 °C (**R_W_300**); b) at 500 °C (**R_W_500**).

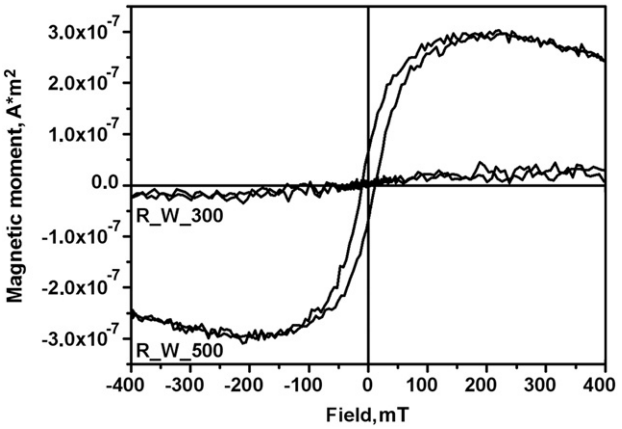

Fig. 5. M(H) at room temperature for the films deposited by water-assisted CVD on r-sapphire substrates at 300 °C (**R_W_300**) and at 500 °C (**R_W_500**).

in the literature for undoped ZnO films [18]. The nanostructured films with whisker structure obtained at 500 °C showed clear ferromagnetic loops. Fig. 5 shows the magnetic hysteresis loop for one of the films (**R_W_500**) with Hc of about 10 mT and a remarkable saturation moment of $3*10^{-7}$ A$*$m^2, which corresponds to a very high specific magnetic moment of 7 A$*$m^2/kg.

Our results indicate that morphology of undoped ZnO films at nano-scale has a strong influence on their magnetic properties. The more developed nanostructure of the film is, the more pronounced is its ferromagnetism. According the hypothesis of Sundaresan et al. [22], FM in undoped ZnO is caused by structure defects located at the surface of nanosized objects. In our work such nano-objects are formed within the ZnO film. If one could learn how to control the film defect structure and the degree of nanocrystallinity in a quantitative manner, it would become possible to control the magnetism in a quantitative manner as well. It is a very difficult task to achieve, however, in the CVD growth of ZnO films, since ZnO has an extremely strong tendency to anisotropic growth, and even minor changes of deposition conditions may result in distinctly different nanostructures.

In order to check the hypothesis mentioned above, we propose another approach to influence the magnetism of epitaxial ZnO films by intentionally introducing nano-sized defects in their structure. Kaul et al. [26] demonstrated that the deposition of ZnO on cubic (111) $MgAl_2O_4$ substrates led to the formation of epitaxial films with in-plane variant structures. On (111) $MgAl_2O_4$ substrates, two equivalent in-plane orientations of ZnO can grow, which differ from each other by a 30° rotation (Fig. 6), in contrast to other substrates where no such in-plane variants form. This leads to the formation of nano-sized variants, or structure domains, each of them is epitaxial in respect to the substrate. XRD data for ZnO films deposited on (111) $MgAl_2O_4$ in oxygen at 600 °C (Fig. 7) confirm out-of plane orientation. φ-scans with periodic reflections at every 30° reveal the variant structure of the films (compare with the φ-scan in Fig. 1 for the film deposited on (111) YSZ).

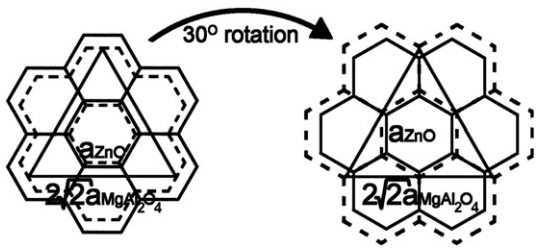

Fig. 6. The scheme of two equivalent in-plane orientations realized at ZnO film growth on (111) $MgAl_2O_4$ substrate. Dotted lines show a stress of the ZnO lattice.

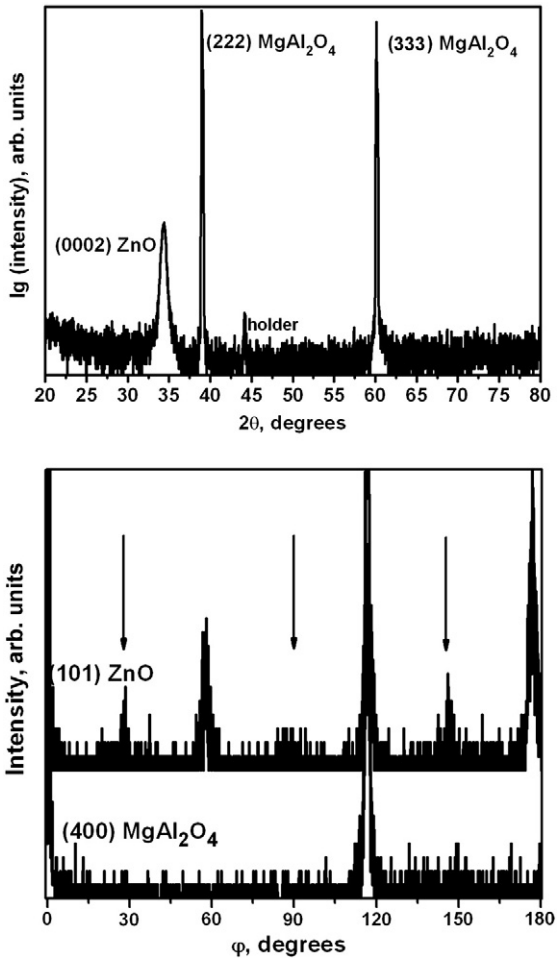

Fig. 7. XRD θ–2θ scan of ZnO film grown on (111) $MgAl_2O_4$ substrate (at the top) and φ-scans for ZnO and (111) $MgAl_2O_4$ (at the bottom).

According to SEM observations, the films on $MgAl_2O_4$ do not possess any special kind of nanostructure at the surface. SEM images of these films are similar to those of epitaxial films on other substrates and therefore are not shown here.). However, the nano-scale imperfections of the epitaxial film structure could be seen in the high-resolution TEM images presented in Fig. 8. Many distorted areas, which start at the interface, penetrate to a film depth of 10–15 nm. They are separated from each other by 15–20 nm. These areas can be interpreted as the structure imperfections at the boundaries of neighboring variants.

The epitaxial ZnO films with variant structure, in contrast to other epitaxial films discussed above, are ferromagnetic at room temperature (Fig. 9). The saturation magnetization is $5*10^{-8}$ A$*$m^2 and $6*10^{-8}$ A$*$m^2 for the films deposited at 600 and 500 °C, respectively, and, similar to the results obtained by Hong at al. [17], the saturation magnetization is much higher for the thin film (50 nm, **MAO_Ox_500**) than that for the thicker film (230 nm, **MAO_Ox_600**). This fact together with the absence of a developed surface nanostructure for this kind of ZnO films allows us to conclude, that in this case the magnetism of the films is most probably caused by introduced structure defects located near the substrate–film interface.

Nanostructure of the films has a strong influence on their electric properties. Films synthesized by water-assisted process at 300 °C with "crossed plates"-like structure had very high, non-measurable resistance, while films with whiskers structure deposited at 500 °C were more conductive and showed values of resistance of about tens MΩ at room temperature. At lower temperatures the resistance was non-

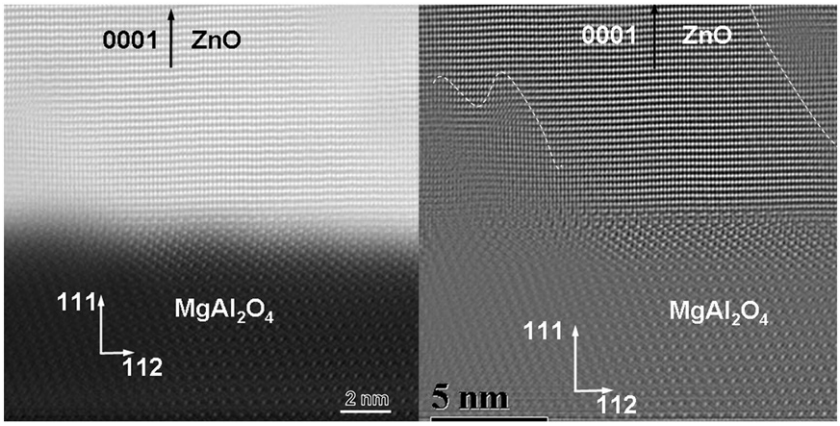

Fig. 8. HRTEM image (left) and its Fourier-transformation (right) for the ZnO film deposited on (111) $MgAl_2O_4$ (**MAO_Ox_600** sample). Thin white lines are shown to mark imperfection areas.

measurable. The temperature dependences of resistivity for the epitaxial films deposited on different substrates in oxygen-containing atmosphere at 600 °C are presented in Fig. 10. All the films investigated showed the behavior typical for semiconductors — resistivity decreased with the increase of the temperature, but resistivity of the films differed by several orders of magnitude depending on the substrate used. ZnO film deposited on (111) $MgAl_2O_4$ showed the highest resistivity. Under the temperature below 150 K the resistivity, ρ, of this film obeyed the Motts law:

$$\rho = \rho_0 e^{(T_0/T)^{1/4}}. \quad (1)$$

Parameter T_0 is close to 2500 K. This is an indication of the hopping mechanism of conductivity in the films deposited on $MgAl_2O_4$. Hopping conductivity points to the localization of the electronic states near Fermi level. Typically, localization of electron states near Fermi level in undoped semiconductors originates from disorder and/or point defects. This is consistent with the structure of the films on (111) $MgAl_2O_4$ substrate, which contains nano-sized defects and imperfections at the boundaries of the variant domains in contrast to the films deposited on other substrates.

In conclusion, undoped ZnO thin films with different nanostructure were obtained by oxygen-assisted and water-assisted CVD. Morphology of the films varied strongly depending on deposition conditions — from dense and rather flat epitaxial films to polycrystalline films with developed nanostructure of whiskers or crossed nano-sized plates. Nanostructure of ZnO films had a crucial influence on their magnetic and electrical properties. The highest magnetic moment possessed ZnO films with highly developed surface deposited at the presence of water vapor at 500 °C. Another way to achieve ferromagnetic undoped ZnO films was the creation of epitaxial variant structure with nanosized structure domains. Our results show, that the conclusion made by Sundaresan et al. [22] about strong correlation between ferromagnetism and nano-sized state of nonmagnetic oxides nanoparticles, extends to the field of thin films.

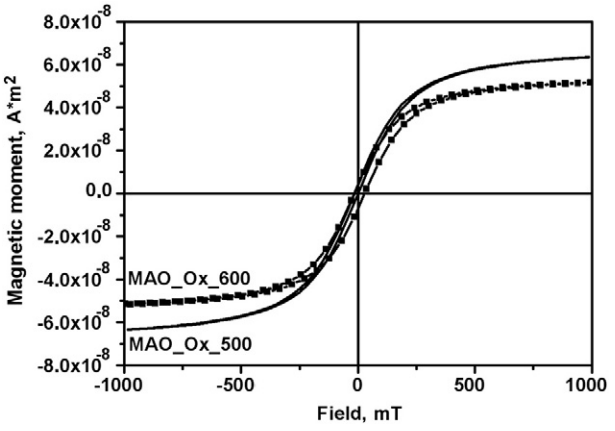

Fig. 9. M(H) at room temperature for the films deposited by oxygen-assisted CVD on (111) $MgAl_2O_4$ substrates at 500 °C (**MAO_Ox_500**) and at 600 °C (**MAO_Ox_600**).

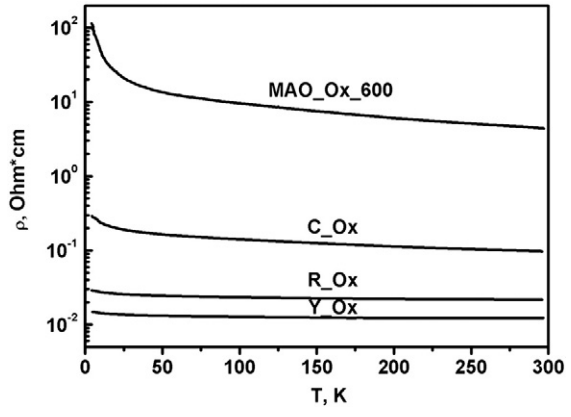

Fig. 10. Temperature dependences of resistivity for the epitaxial ZnO films deposited at 600 °C by oxygen-assisted CVD on different substrates.

Acknowledgments

The authors are grateful to Dr. A.A. Kamenev for SEM investigations and Dr. V.A. Amelichev for XRD measurements. This work was partly supported by RFBR program no. 09-03-00942-a, and Lidia Burova's participation at EMRS-2011 Spring Meeting was supported by RFBR travel grant no. 11-03-09263-mob-z.

References

[1] T. Dietl, H. Ohno, F. Matsukura, J. Cibert, D. Ferrand, Science 87 (2000) 1019.
[2] P. Sharma, A. Gupta, K.V. Rao, F.J. Owens, R. Sharma, R. Ahuja, J.M. Osorio Guillen, B. Johansson, G.A. Gehring, Nat. Mater. 2 (2003) 673.
[3] M. Venkatesan, C.B. Fitzgerald, J.G. Lunney, J.M.D. Coey, Phys. Rev. Lett. 93 (2004) 177206.
[4] Ü. Özgür, Ya.I. Alivov, C. Liu, A. Teke, M.A. Reshchikov, S. Doğan, V. Avrutin, S.-J. Cho, H. Morkoç, J. Appl. Phys. 98 (2005) 041301.
[5] T.S. Herng, S.P. Lau, S.F. Yu, H.Y. Yang, L. Wang, M. Tanemura, J.S. Chen, Appl. Phys. Lett. 90 (2007) 032509.

[6] V.G. Kytin, V.A. Kulbachinskii, D.S. Glebov, L.I. Burova, A.R. Kaul, O.V. Reukova, Semiconductors 44 (2010) 164.
[7] J. Alaria, H. Bieber, S. Colis, G. Schmerber, A. Dinia, Appl. Phys. Lett. 88 (2006) 112503.
[8] K. Potzger, S. Zhou, Phys. Status Solidi B 246 (2009) 1147.
[9] N.A. Spaldin, Phys. Rev. B 69 (2004) 125201.
[10] A. Waag, in: C.F. Klingshirn, B.K. Meyer, A. Waag, A. Hoffmann, J. Geurts (Eds.), Zinc Oxide: From Fundamental Properties Towards Novel Applications, Springer-Verlag Berlin Heidelberg, 2010, p. 267.
[11] L.I. Burova, S.V. Samoilenkov, M. Fonin, E. Biegger, Y. Dedkov, E.A. Ganshina, O.Y. Gorbenko, U. Rüdiger, A.R. Kaul, Thin Solid Fims 515 (2007) 8490.
[12] S.-W. Lim, M.-C. Jeong, M.-H. Ham, J.-M. Myoung, Jpn. J. Appl. Phys. 43 (2004) L280.
[13] M. Diaconu, H. Schmidt, H. Hochmuth, M. Lorenz, G. Benndorf, D. Spemann, A. Setzer, P. Esquinazi, H. von Wenckstern, R. Gross, H. Schmid, W. Mader, G. Wagner, M. Grundmann, J. Magn. Magn. Mater 307 (2006) 212.
[14] S.J. Han, T.H. Jang, Y.B. Kim, B.G. Park, J.H. Park, Y.H. Jeong, Appl. Phys. Lett. 83 (2003) 920.
[15] S.W. Yoon, S.-B. Cho, S.C. We, S. Yoon, B.J. Suh, H.K. Song, J. Appl. Phys. 93 (2003) 7879.
[16] B.B. Straumal, S.G. Protasova, A.A. Mazilkin, A.A. Myatiev, P.B. Straumal, G. Schütz, E. Goering, B. Baretzky, J. Appl. Phys. 108 (2010) 073923.
[17] N.H. Hong, J. Sakai, V. Briz'e, J. Phys.: Condens. Matter 19 (2007) 036219.
[18] M. Kapilashrami, J. Xu, V. Ström, K.V. Rao, L. Belova, Appl. Phys. Lett. 95 (2009) 033104.
[19] Q. Xu, H. Schmidt, S. Zhou, K. Potzger, M. Helm, H. Hochmuth, M. Lorenz, A. Setzer, P. Esquinazi, C. Meinecke, M. Grundmann, Appl. Phys. Lett. 92 (2008) 082508.
[20] D. Gao, Z. Zhang, J. Fu, Y. Xu, J. Qi, D. Xue, J. Appl. Phys. 105 (2009) 113928.
[21] Z. Yan, Y. Ma, D. Wang, J. Wang, Z. Gao, L. Wang, P. Yu, T. Song, Appl. Phys. Lett. 92 (2008) 081911.
[22] A. Sundaresan, R. Bhargavi, N. Rangarajan, U.R. Siddesh, C.N.R. Rao, Phys. Rev. B 74 (2006) 161306.
[23] A. Sundaresan, C.N.R. Rao, Nano Today 4 (2009) 96.
[24] B.B. Straumal, F.F. Mazilkin, S.G. Protasova, A.A. Myatiev, P.B. Straumal, G. Schütz, P.A. van Aken, E. Goering, B. Baretzky, Phys. Rev. B 79 (2009) 205206.
[25] S.V. Samoylenkov, O.Yu. Gorbenko, I.E. Graboy, A.R. Kaul, Yu.D. Tretyakov, J. Mater. Chem. 6 (1996) 623.
[26] A.R. Kaul, O.Y. Gorbenko, A.N. Botev, L.I. Burova, Superlattices Microstruct. 38 (2005) 272.